



## Original article

## Novel 3,3'-diindolylmethane derivatives: Synthesis and cytotoxicity, structural characterization in solid state

Dorota Maciejewska<sup>a,\*</sup>, Magdalena Rasztańska<sup>a</sup>, Irena Wolska<sup>b</sup>,  
Elżbieta Anuszevska<sup>c,\*\*</sup>, Beata Gruber<sup>c</sup>

<sup>a</sup> Department of Organic Chemistry, Faculty of Pharmacy, Medical University of Warsaw, 1 Banacha Str, 02 097 Warsaw, Poland

<sup>b</sup> Department of Crystallography, Faculty of Chemistry, Adam Mickiewicz University, 6 Grunwaldzka Str, 60-780 Poznań, Poland

<sup>c</sup> Department of Biochemistry and Biopharmaceuticals, National Medicines Institute, 30/34 Chelmska Str, 00-725 Warsaw, Poland

## ARTICLE INFO

## Article history:

Received 6 March 2009

Received in revised form

4 May 2009

Accepted 7 May 2009

Available online 22 May 2009

## Keywords:

3,3'-Diindolylmethane derivatives

<sup>13</sup>C CP/MAS NMR

X-ray diffraction

Cytotoxicity

## ABSTRACT

A series of 3,3'-diindolylmethane derivatives have been synthesized and their structures were characterized in solid state by <sup>13</sup>C CP/MAS NMR and two of them by X-ray diffraction measurements. They exhibited well expressed cytotoxicity against human melanoma cell lines. Derivatives bearing fluoro, bromo, iodo, and nitro substituents in indole or benzene rings caused 50% inhibition of the viability of ME18 and ME18/R cell lines at concentration ranging 9.7–17.3 μM.

© 2009 Elsevier Masson SAS. All rights reserved.

### 1. Introduction

3,3'-Diindolylmethane is considered to be a promising anti-tumor agent derived from *Brassica* food plants (cabbage, broccoli, Brussels sprouts, cauliflower), which could protect against tumorigenesis in multiple organs (forestomach, mammary gland, uterus, liver). However, such phytonutrients may exhibit adverse promoting activity in certain test protocol or in other organs [1,2]. 3,3'-Diindolylmethane has reached an important position in the research works aimed at understanding the mechanisms of anti-proliferative processes in tumor cell lines, especially in human breast cancer cells [3–10]. 3,3'-Diindolylmethane induced a G<sub>1</sub> cell cycle arrest in human breast cancer, regardless of their estrogen receptor or p53 tumor suppressor status, by an increase in expression of the CDK inhibitor, p21<sup>Cip1/Waf1</sup>. Further investigations showed that 3,3'-diindolylmethane is a strong mitochondrial H<sup>+</sup>-ATPase inhibitor, and stimulates mitochondrial reactive oxygen species (ROS) production, which leads to processes involving the stress-activated protein kinases, c-Jun NH<sub>2</sub>-terminal and p38. As

a result, it was established that an enhancement of mitochondrial release of ROS is responsible for p21 up-regulation. 3,3'-Diindolylmethane was found to have low bioavailability, what have limited its possible widespread use. The discovery of an absorbable form of 3,3'-diindolylmethane [11] allowed the use of a potency of this compound. Recent reports show that the highly absorbable microencapsulated formulation of 3,3'-diindolylmethane is in I/III phases of clinical trials for treatment of cervical dysplasia and prostate cancer. This formulation is also used for promotion of healthy estrogen metabolism. These make the *bis*-indoles an important class of anticancer chemotherapeutics and potential source of medicinal lead compounds. Methods of their synthesis are still developed [12–19]. Taking into account all the facts we synthesized ten new 3,3'-diindolylmethanes (Fig. 1) and studied their antiproliferative potential against normal cells and two human melanoma cells.

In the present work we report also the single crystal X-ray diffraction measurements as well as the analysis of <sup>13</sup>C CP/MAS NMR spectra in solid state. We are hopeful that structural analysis of the title compounds in solid state can provide useful information for further development of our work. Examinations of the structures of the designed compounds could be essential for obtaining experimental parameters, which can become descriptors in the planned structure–activity studies.

\* Corresponding author. Tel./fax: +48 022 5720 643.

\*\* Corresponding author.

E-mail addresses: [domac@farm.amwaw.edu.pl](mailto:domac@farm.amwaw.edu.pl) (D. Maciejewska), [anuszevska@il.waw.pl](mailto:anuszevska@il.waw.pl) (E. Anuszevska).

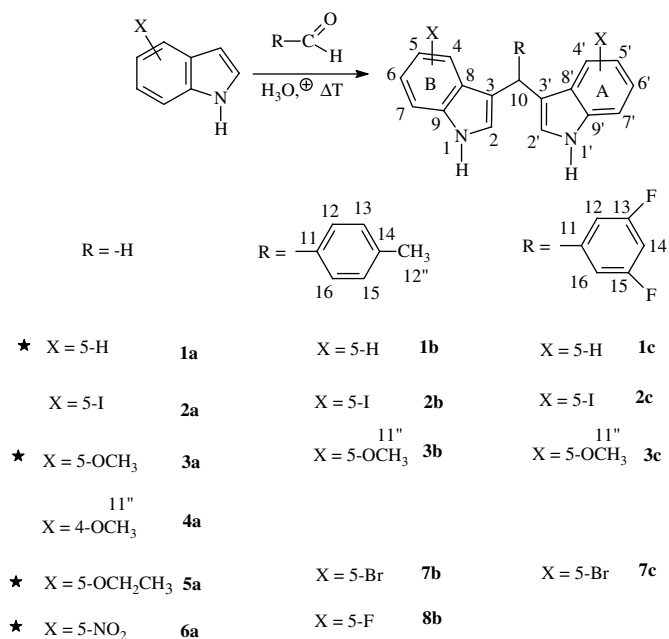


**Fig. 1.** General synthetic pathway together with compounds and atom numbering. Structural data for compounds marked with asterisk (\*) were already published by us.

## 2. Results and discussion

### 2.1. Chemistry

The principal synthetic route to the *bis*-indolylmethanes is the condensation of corresponding indole derivatives with aliphatic or aromatic aldehydes in the acidic medium (Fig. 1). We made some modifications of the standard procedure, which are reported in the [Experimental part](#). Standard 1D and 2D hetero- and homomolecular <sup>1</sup>H and <sup>13</sup>C NMR experiments in CDCl<sub>3</sub> or DMSO-*d*<sub>6</sub> were sufficient to characterize the studied compounds in solution. Complete assignments of the solution resonances are given in Section 4.

### 2.2. <sup>13</sup>C CP/MAS NMR spectra in solid state

From the 1960s the interest in polymorphism of drugs (bound with the bioavailability of their form) developed among the pharmaceutical community [20–22], and continues to be, particularly in the development of new drug entities or new active substances obtained in laboratory. <sup>13</sup>CP/MAS NMR spectra of powdered samples are very useful for characterization of the solid state structure of organic compounds [23]. The <sup>13</sup>C NMR experimental resonances could be combined with the theoretical values in an attempt to predict stable conformations present in the solid state together with the intramolecular interactions. Some chemical species, which are employed for such analyses, may soon be used for generating new pharmaceutical solids with desirable properties.

Exemplary solid state <sup>13</sup>C CP/MAS NMR spectra are shown in [Figs. 2 and 3](#) and the most probable assignments of resonances are given in [Table 1](#). In [Fig. 2](#) we have presented two spectra of type-**a** derivatives (without an additional aromatic ring): 5,5'-diiodo-3,3'-diindolylmethane (**2a**) and the 4,4'-dimethoxy-3,3'-diindolylmethane (**4a**). Below these two, the spectra of type-**b** derivatives are shown (type-**b** derivatives have 4-methylphenyl ring): 5,5'-dimethoxy-3,3'-diindolyl-(4-methylphenyl)methane (**3b**), and 5,5'-difluoro-3,3'-diindolyl-(4-methylphenyl)methane (**8b**). In [Fig. 3](#) we have shown the spectra of four derivatives of type **c**, having 3,5-difluorophenyl ring: the

3,3'-diindolyl-(3,5-difluorophenyl)methane (**1c**), the 5,5'-diiodo-3,3'-diindolyl-(3,5-difluorophenyl)methane (**2c**), the 5,5'-dimethoxy-3,3'-diindolyl-(3,5-difluorophenyl)methane (**3c**), and the 5,5'-dibromo-3,3'-diindolyl-(3,5-difluorophenyl)methane (**7c**). All examined molecules have two identically substituted indolyl moieties and for the chemically equivalent pairs of atoms from both indole systems we have observed a different pattern of NMR resonances in the solid state: for compounds **2a**, **2b**, **8b** and **1c**, **2c**, **7c**, the simple solution-like spectra but for compounds **4a**, **1b**, **3b** and **3c** more complicated, double signals' pattern for majority of atoms.

There could be several reasons for these differences. The solution-like spectrum is favored in case, when the intermolecular interaction does not dominate. The double resonances could be caused by i) the presence of two energetically similar conformers in solid state (polymorphism), ii) the co-crystallization with solvent (pseudopolymorphism) or iii) different packing mode of both indole rings in one conformer. Certainly, spin–spin coupling of <sup>19</sup>F and <sup>14</sup>N atoms with <sup>13</sup>C atoms also could be observed.

The experimental chemical shifts  $\delta$  [ppm] were compared with the theoretical shielding constants  $\sigma$  [ppm] computed at DFT level employing B3LYP/6-311G (d, p) hybrid functional and CPHF-GIAO approach for low energy conformers (obtained at PM3 level of theory) for all compounds apart from these with I-atoms (I atom is not well parameterized within Gaussian 03). These calculations helped us to assign properly the <sup>13</sup>C NMR resonances and provided insight into the structural features of the examined compounds in solid state. Moreover, we determined the geometries of **2a** and **8b** by X-ray analysis and compared the obtained conformation of **8b** with its spectroscopic NMR data in solid state, computing the <sup>13</sup>C shielding constants  $\sigma$  [ppm] for X-ray derived atomic coordinates. Simultaneously, using the same method we computed the shielding constants for PM3 geometry of **8a**. We have found linear correlations between theoretical  $\sigma$  values and the experimental chemical shifts  $\delta$  [ppm] for both atomic coordinates. The above finding is good evidence that linear correlations between the computed shielding constants for PM3 geometries and the experimental chemical shifts could be used to analyze the molecular structure of the studied *bis*-indoles.

In the spectra of compounds of **1b**, **8b**, **2c**, **7c** the strong signal in the vicinity of 129 ppm was measured. It arises from the inclusion of benzene molecule into the crystallographic net. The interactions between benzene and indole rings seem to be responsible for splitting the resonances of <sup>13</sup>C atoms of indole systems in the spectra of **1b** and **8b**. This is not revealed in the spectra of **2c** and **7c**. For the methoxy derivatives (**4a**, **3b**, **3c**) spectral analysis disclosed double signals of <sup>13</sup>C atoms of both indole rings, as was evidenced previously by us for resemble compounds [24,25]. The methoxy substituents at C5, C5' atoms of indole rings in compounds **3b**, **3c** are situated in aromatic rings' plane, and are oriented in such a way that methyl groups point at C4 or C4' atoms. This is confirmed by upfield shifts of these atoms' resonances in solid state as compared to solution one. Similarly, methoxy groups at C4, C4' atoms indole rings are located in the plane of the aromatic rings, and upfield shifts of C5 (C5') resonances are observed. The dihedral angles formed by methoxy groups and indole rings (C11''–O–C5–C4, C11''–O–C4'–C5', C11''–O–C4–C6, C11''–O–C4'–C6') are slightly different, resulting in various values of shielding constants of <sup>13</sup>C atoms in indole rings, and as a consequence the <sup>13</sup>C resonances are doubled. The effect of halogen substituents at indole ring is not so significant on the geometry of examined compounds (see exemplary spectra of **2a**, **8b**, **2c**, **7c**). The packing of these molecules is stabilized by different type of symmetric weak intermolecular interactions which slightly shift downfield the <sup>13</sup>C NMR resonances as referenced to solution one. The peak multiplicities and intensity of the resonances are in agreement with the solution spectra. Only the

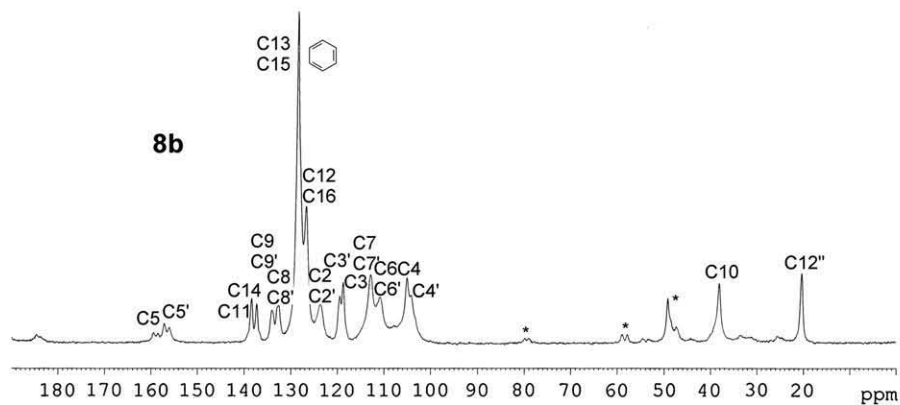
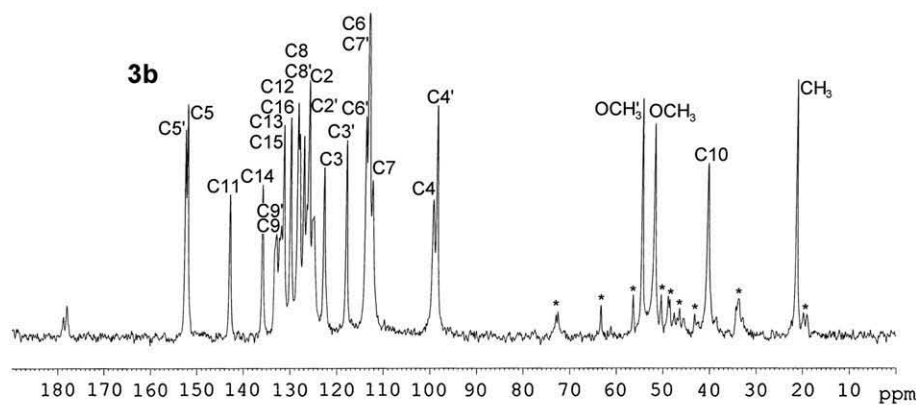
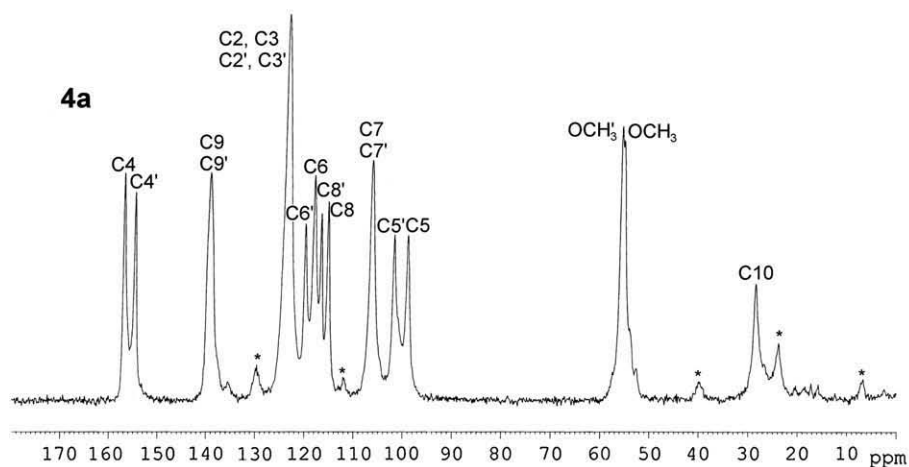
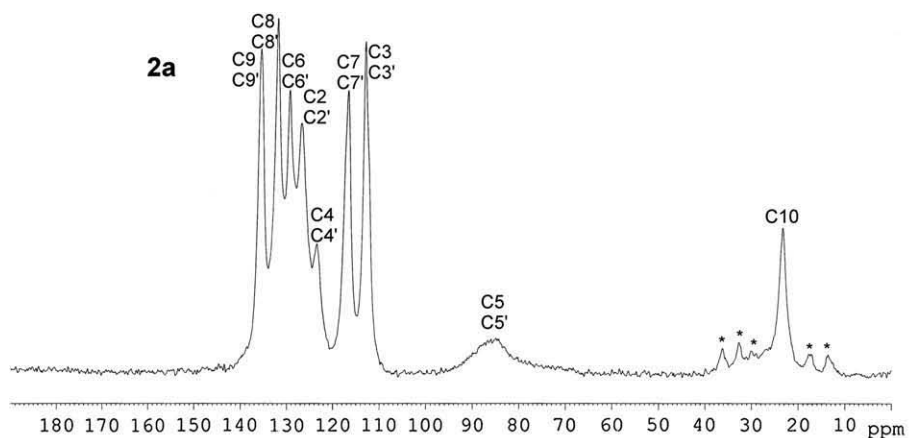


**Fig. 2.** The  $^{13}\text{C}$  CP/MAS NMR spectra of **2a**, **4a**, **3b** and **8b** in the solid state. Sidebands are marked with an asterisk.

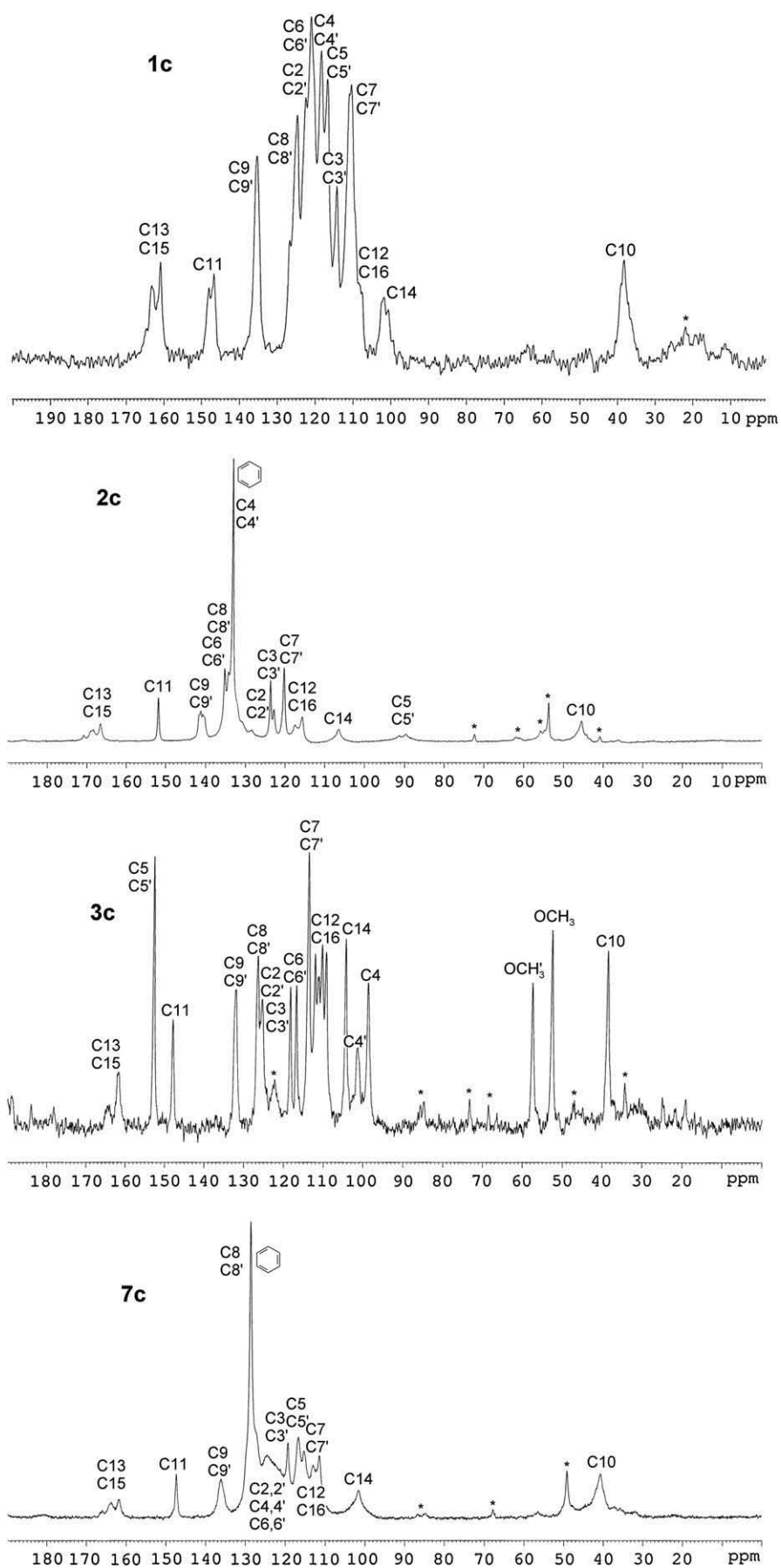


Fig. 3. The  $^{13}\text{C}$  CP/MAS NMR spectra of **1c**, **2c**, **3c** and **7c** in the solid state. Sidebands are marked with an asterisk.

**Table 1**  
Assignments of resonances in  $^{13}\text{C}$  CP/MAS NMR spectra of studied compounds.

No	Chemical shifts of $^{13}\text{C}$ in solid state, $\delta$ [ppm]								
	$^{13}\text{C}$ atoms numbering								
	C2;C2'	C3;C3'	C4;C4'	C5;C5'	C6;C6'	C7;C7'	C8;C8'	C9;C9'	The rest of signals
<b>2a</b>	126.9	113.1	123.6	85.0 (broad)	129.5	116.8	132.1	135.7	23.5-C10
<b>4a</b>	123.4	123.4	157.0 154.7	101.9 99.1	119.9 118.1	106.4	116.7 115.5	139.3	23.9-C10; 55.8, 55.4-C-11*
<b>1b</b>	123.9	116.9	118.4	112.2	120.4	110.9	127.1	136.0	38.1-C-10; 19.5-C12*; 139.7-C11, 129.2-C12, 16; 130.2-C13, 15; 137.2-C14 (broad)
<b>2b</b>	123.4 123.3	117.4	119.1 128.5	88 (broad)	121.5 131.5	112.6	127.6 130.3	135.6	39.7-C-10; 22.0-C12*; 140.6-C11, 128.7-C12, 16; C13, 15; 136.3-C14
<b>3b</b>	125.0	118.0	98.6	152.1	113.3	112.4	127.2	131.9	40.4-C-10; 21.4-C12*; 51.9, 54.5-C11*, 142.9-C11, 130.0-C12, 16; 131.4-C13, 15; 136.0-C14
<b>7b</b>	126.0 124.7	122.8 117.2	99.4 122.5	152.5 112.8	113.9 124.7	113.3 112.8	128.1 129.5	133.0 135.1	39.1-C-10; 20.9-C12*; 140.0-C11, 127.6-C12, 16; 129.5-C13, 15; 134.9-C14
<b>8b</b>	123.8	119.6 118.9	105.2 104.2	159.0 156.6	110.9	113.0	132.8	134.1	38.3-C-10; 20.5-C12*; 138.5-C11, 126.9-C12, 16; 128.8-C13, 15; 137.4-C14
<b>1c</b>	122.7	114.6	117.2	118.9	121.6	110.9	125.1	135.6	38.5-C10; 147.5-C11; 110.9-C12, 16; 162.1-C13, 15; 101.9-C14
<b>2c</b>	123.7	122.8	133.2	89.7 (with benzene)	135.2 (broad)	120.3	133.2	141.2	45.4-C10; 151.9-C11; 116.6-C12, 16; 168.4-C13, 15; 106.5-C14
<b>3c</b>	124.0	116.9	97.3 99.8	151.3	115.4	112.4	125.1	130.8	37.3-C10; 56.1, 51.3-C11''; 146.5-C11; 109.3-C12, 16; 161.5-C13, 15 99.9-C14
<b>7c</b>	124.5 (broad)	119.3	124.5 (broad)	116.7	124.5 (broad)	113.1	128.7 (with benzene)	136.2	40.8-C10; 147.4-C11; 92.3-C12, 16; 163.8-C13, 15 101.7-C14

spectrum of fluoroindole derivative **8b** (with F atoms at C5, C5' positions, third aromatic ring and benzene molecule included in the crystallographic net) consists of double peaks due to the two distinct indole moieties. The spectra of compounds having F atoms show a number of splitted resonances of  $^{13}\text{C}$  atoms proximal to F atoms due to spin–spin coupling between  $^{13}\text{C}$  and  $^{19}\text{F}$  atoms. On the other hand, the effect of phenyl ring (derivatives of types **b** and **c**) on the spatial orientation of two indole systems is not significant. The angles formed by the bonds at the central C10 atom are close to  $110^\circ$ , which means that they are similar to the standard tetrahedral  $109^\circ$ . The solid state forms of derivatives' types **a** and **b** can change according to the medium used for crystallization. The solvent may interact with the solute leading to the formation of mixed crystals. In this work, such phenomenon was observed for compounds **1b**, **8b**, **2c**, **7c**, which were solvated by benzene used in synthetic procedure. The exemplary geometries in solid state determined on the basis of  $^{13}\text{C}$  CP/MAS NMR and molecular modeling are shown in Fig. 4: for compound **4a** (as an example of derivatives of type **a**), for compound **7b** (as an example of derivatives of type **b**) and for compound **1c** (as an example of derivatives of type **c**).

### 2.3. Crystal structures of 5,5'-diiodo-3,3'-diindolylmethane **2a** and 5,5'-difluoro-3,3'-diindolyl(4-methylphenyl)methane **8b**

The molecular and crystal structures of **2a** and **8b** in solid state were analyzed by single crystal X-ray diffraction. The displacement ellipsoid representation of the molecules, together with the atomic numbering scheme, is shown in Fig. 5 (the drawings were performed with Mercury program [26]).

Both compounds crystallize in the monoclinic space group  $P2_1/n$  with a single molecule in the asymmetric unit. Moreover the crystals of **8b** include the disordered solvent molecule in such unit. The structures consist of two indole systems connected by a common C atom (C10), different halogen atoms at C5, and compound **8b** has additional aromatic 4-methylphenyl ring at C10.

Selected bond lengths, bond angles and torsion angles are listed in Table 2.

The conformations of the molecules are very similar. The indole fragments are essentially planar to within  $0.020(3)$  Å for **2a** and  $0.013(3)$  Å for **8b** with the dihedral angle between their mean planes of  $89.67(6)^\circ$  and  $86.38(7)^\circ$  for **2a** and **8b**, respectively. The arrangement of these fragments can be described by the torsion angle C8–C3–C10–C3' (see Table 2). The halogen atoms are nearly coplanar with the two-ring frameworks. In **8b**, the disposition of the planar 4-methylphenyl ring at C10 with respect to the indole fragments can be described by the torsion angles C2–C3–C10–C11 of  $-108.3(3)^\circ$  and C2';–C3';–C10–C11 of  $31.9(4)^\circ$ .

In the crystals, the packing of the molecules is stabilized by dissimilar weak intermolecular interactions. The geometric parameters of all these bonds are given in Table 3.

The crystal structure of **2a** is built of layers of the molecules parallel to (10–1) plane. Within the layer the molecules are connected via N1–H1 $\cdots\pi$  and N1'–H1' $\cdots$ C7 hydrogen bonds (Fig. 6). The consecutive inversion centers connect the molecules from adjacent layers. Short contacts C10 $\cdots$ C10 and C2 $\cdots$ I' between the layers result from the crystal packing of the molecules. The packing arrangement is shown in Fig. 7.

In the crystal of **8b**, there is a three dimensional network of hydrogen-bonding interactions. The molecules are linked by C6–H6 $\cdots$ F', C1B–H1B $\cdots$ F and N1'–H1' $\cdots$ C6 hydrogen bonds forming layers parallel to (001) plane (Fig. 8). Cohesion between the layers results from the N1–H1 $\cdots\pi$  contacts (Fig. 9). The packing arrangement along the *b* axis (Fig. 10) shows the benzene molecules inside the canals parallel to [101] direction.

### 2.4. Cytotoxic activity of bis-indoles

Compounds **3a**, **6a** and **1c**, **3c** were submitted to the National Cancer Institute for testing against panel of 60 cancer lines. Details of **3a**, **6a** tests were published [24,27]. Compounds **1c** and **3c** were evaluated at concentration of 10  $\mu\text{M}$  against a panel of nine cancer

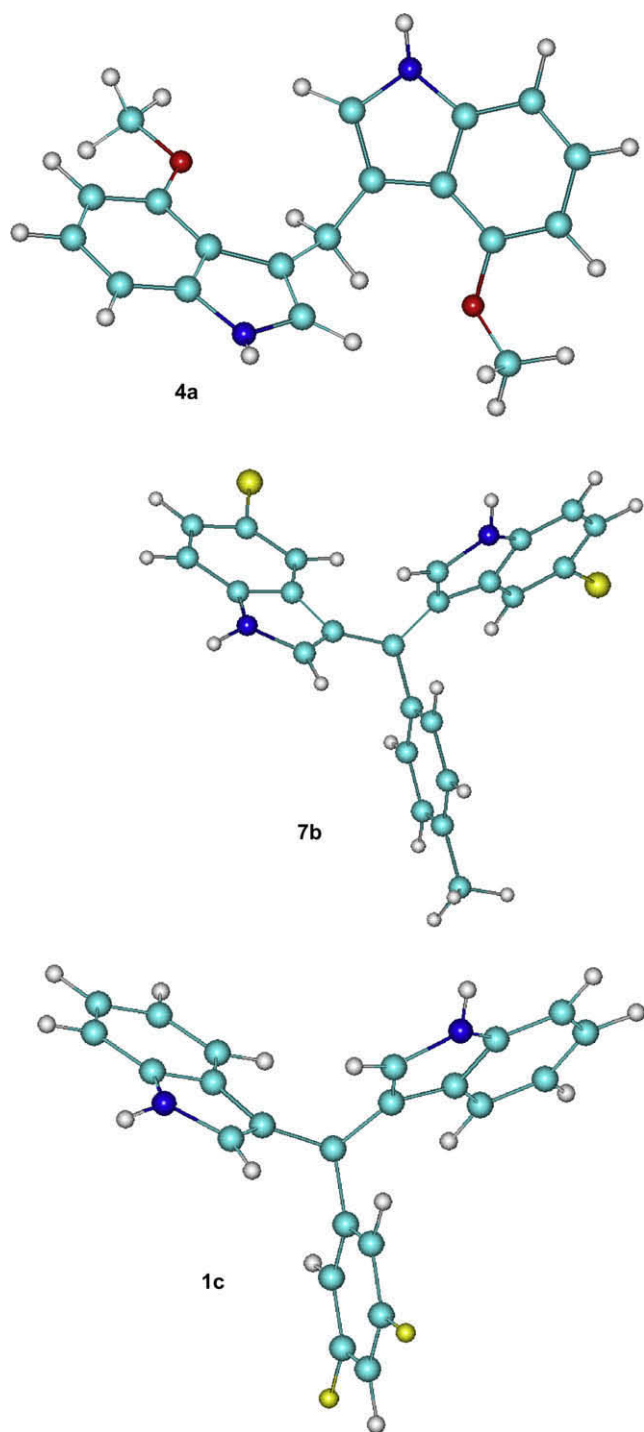


Fig. 4. Hypothetical conformations in solid state shown for **4a**, **7b** and **1c** as the representatives of three types of analyzed compounds.

cell lines: leukemia, non-small cell lung, colon, CNS, melanoma, ovarian, renal, prostate and breast. Both inhibited strongly growth of ovarian cancer line IGROV1 (−6.52 and −7.10%, respectively), moderately inhibited growth of renal cancer line UO-31 (52.86 and 43.23%, respectively), melanoma line SK-MEL-2 (58.84 and 62.49%, respectively), and prostate cancer line PC-3 (67.07 and 50.16%, respectively). Simultaneously, it was noted that compounds **1c** and **3c** increased growth of some cancer lines, particularly melanoma MALME-3M cancer line. To obtain more detailed information about

biological activities of *bis*-indoles, we examined their cytotoxicities on two human melanoma cell lines ME18 and ME18/R (resistant to doxorubicin) and compared them with that of the human embryonic skin fibroblasts WS1. Sensitivity of cells to *bis*-indole derivatives was defined on the basis of  $IC_{50}$  values obtained in MTT assay in the concentrations ranging from 1.25 to 30  $\mu\text{g/ml}$ . The  $IC_{50}$  values were determined as the concentration of tested compounds decreasing cell density to 50% as compared to that in the untreated culture after incubation time. Table 5 summarizes the cytotoxicity data. The tested *bis*-indoles demonstrated cytotoxic effects for both human melanoma cell lines ME18 and ME18/R. 5,5'-Dithio-3,3'-diindolylmethane (**2a**), 5,5'-dinitro-3,3'-diindolylmethane (**6a**) and 5,5'-dibromo-3,3'-diindolyl(4-methylphenyl)methane (**7b**) proved to be the most active cytotoxic agents amongst the studied compounds. 3,3'-Diindolyl(3,5-difluorophenyl)methane (**1c**) was characterized by higher activity against ME18/R cell lines, resistant to doxorubicin. Compounds **2b**, **2c**, **3c**, and **7c** were found to be practically equipotent. Derivative **1b** displayed the least pronounced cytotoxic effect.

The cytotoxicity determination was extended to human embryonic skin fibroblasts cell line WS1, chosen as representative for normal, non-malignant cellular population. As was evidenced most of the *bis*-indoles (**4a**, **5a**, **6a**, **1b**, **3b**, **7b**, **8b**, **1c**, **2c** and **7c**) were less cytotoxic against WS1 cells as compared to the human melanoma cell lines. Comparable sensitivity of normal fibroblasts and neoplastic cells – ME18 was noted in the case of **3a** which occurred as less cytotoxic to ME18/R cells. The reference agent 3,3'-diindolylmethane **1a** exhibited the similar effectiveness towards WS1, comparable to its effects towards ME18 and ME18/R cells.

The following derivatives: 5,5'-dinitro-3,3'-diindolylmethane (**6a**), 5,5'-diethoxy-3,3'-diindolylmethane (**5a**) and 4,4'-dimethoxy-3,3'-diindolylmethane (**4a**) occurred to be the most interesting compounds. They were cytotoxic to ME18/R as well as to ME18 but not cytotoxic to normal human fibroblasts WS1. Among the tricyclic derivatives of types **b** and **c** we chose three of them which deserve further testing, i.e., 3,3'-diindolyl(3,5-difluorophenyl)methane **1c** > 5,5'-dibromo-3,3'-diindolyl(4-methylphenyl)methane (**7b**) > 5,5'-dithio-3,3'-diindolyl(4-methylphenyl)methane (**2b**).

### 3. Conclusion

The most interesting compounds, i.e. cytotoxic to human melanoma ME18/R and ME18 cell lines but not cytotoxic to normal human fibroblasts WS1 appeared to be the following derivatives: 5,5'-dinitro-3,3'-diindolylmethane (**6a**), 5,5'-diethoxy-3,3'-diindolylmethane (**5a**) and 4,4'-dimethoxy-3,3'-diindolylmethane (**4a**). All studied derivatives of 3,3'-diindolylmethane existed in solid state as single molecules in an independent unit, and splitting of resonances in  $^{13}\text{C}$  CP/MAS NMR spectra is due to different packing mode of both indole rings in one conformer. The conformations of the alkoxy substituents are crucial for the observed spectral pattern. As concluded from X-ray diffraction measurement within the layer the molecules are connected via  $\text{N1}\cdots\text{H1}\cdots\pi$  and  $\text{N1}'\cdots\text{H1}'\cdots\text{C}$ -indole interactions. The halogens located at indole and phenyl rings are engaged in several intermolecular interactions for example between  $\text{C2}\cdots\text{I}'$ ,  $\text{C6}\cdots\text{H6}\cdots\text{F}'$  and  $\text{C1B}\cdots\text{H1B}\cdots\text{F}$ .

### 4. Experimental

All chemicals were purchased from major chemical suppliers as high or highest purity grade and used without further purification.

Melting points (mp) were determined with a Digital Melting Point Apparatus 9001 and are uncorrected. Elemental analyses

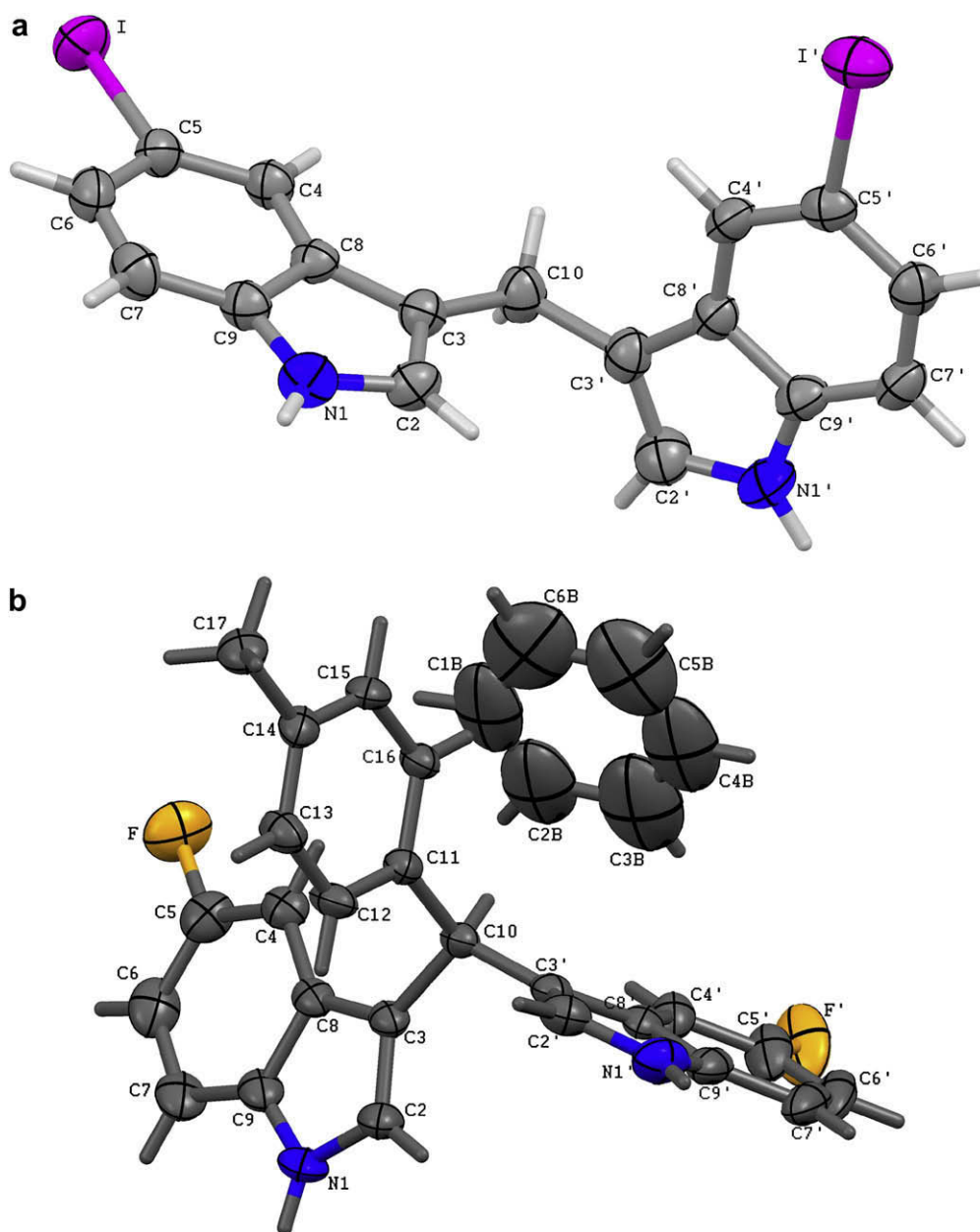


Fig. 5. The molecular structures of **2a** (a) and **8b** with the benzene molecule (b).

were performed on GmbH – Vario EL III C,H,N,S Element Analyzer, and were averaged from two independent determinations.

$^1\text{H}$  NMR and  $^{13}\text{C}$  NMR spectra in solution were recorded at 25 °C with a Bruker Avance DMX 400 spectrometer. Several (as indicated)  $^1\text{H}$  NMR and  $^{13}\text{C}$  NMR spectra in solutions were recorded with a Varian Unity plus-500 or Varian VNMRS-300 spectrometers. The  $^{13}\text{C}$  CP/MAS NMR spectra in solid state were recorded with a Bruker Avance DMX 400 spectrometer. Samples were contained in 4 mm  $\text{ZrO}_2$  rotors and mounted in standard 4 mm MAS probe, and were spun at 8 kHz. A contact time of 4 ms, a repetition time of 20 s, and spectral width of 24 kHz were used for accumulation of 2000–4000 scans. Nonprotonated carbons were selectively observed by dipolar-dephasing experiment with delay time 50  $\mu\text{s}$ . Chemical shifts [ppm] were referenced to TMS. The notation used in the NMR assignments is given in Fig. 1.

Both crystallographic and optimized atom coordinates for **8b** and optimized for remaining compounds were used for

Table 2

Selected bond lengths [Å] and angles [°] and selected torsional angles [deg] for **2a** and **8b**.

	<b>2a</b>	<b>8b</b>
N1–C9	1.360(5)	1.395(4)
N1'–C9'	1.369(4)	1.368(4)
N1–C2	1.372(4)	1.389(4)
N1'–C2'	1.369(5)	1.396(4)
C8–C9	1.408(4)	1.435(4)
C8'–C9'	1.412(4)	1.421(4)
C3–C10	1.503(5)	1.533(4)
C3'–C10'	1.505(5)	1.533(4)
C9–N1–C2	108.8(2)	108.4(2)
C9'–N1'–C2'	109.3(3)	110.0(2)
C3–C10–C3'	115.9(3)	111.4(2)
C8–C3–C10–C3'	177.7(3)	–162.4(2)
C8'–C3'–C10–C3	–89.5(4)	83.6(3)
N1–C2–C3–C10	–178.5(3)	177.0(2)
N1'–C2'–C3'–C10'	176.7(3)	179.1(2)

**Table 3**  
Hydrogen-bonding geometry [Å and °] for **2a** and **8b**. Intermolecular interactions in crystals (Å, °).

D–H...A	d(D–H)	d(H...A)	d(D...A)	<(DHA)
<b>2a</b>				
N1'–H1'...C7 <sup>i</sup>	0.86	2.82	3.579(4)	148
N1–H1...Cg <sup>ii</sup>	0.86	2.76	3.538(9)	151
C10...C10 <sup>iii</sup>			3.367(7)	
C2...I <sup>iv</sup>			3.620(3)	
<b>8b</b>				
C6–H6...F <sup>i</sup>	0.93	2.33	3.194(4)	154
C1B–H1BA...F <sup>ii</sup>	0.93	2.56	3.381(8)	148
N1'–H1'...C6 <sup>iii</sup>	0.86	2.84	3.622(4)	153
N1–H1...Cg <sup>iv</sup>	0.86	2.70	3.507(9)	157

C<sub>g</sub> in upper part of the table represents the centroid of six-membered ring C4'/C5'/C6'/C7'/C8'/C9' of the indole. Symmetry codes (upper part of the table): (i) 1/2 + x, 1/2 – y, 1/2 + z; (ii) x, –1 + y, z; (iii) 1 – x, 1 – y, 1 – z; (iv) –x, 1 – y, 1 – z. C<sub>g</sub> in lower part of the table represents the centroid of five-membered ring N1'/C2'/C3'/C8'/C9' of the indole. Symmetry codes (lower part of the table): (i) 3/2 – x, –1/2 + y, 3/2 – z; (ii) 1 – x, –y, 1 – z; (iii) 1/2 – x, 1/2 + y, 3/2 – z; (iv) 1/2 + x, 1/2 – y, 1/2 + z.

computation of shielding constants  $\sigma$  [ppm] of <sup>13</sup>C atoms to assign the resonances in solid state NMR spectra. We have employed the PM3 semiempirical method for structures' optimization [28] and the DFT method with B3LYP/6-311G (d, p) hybrid functional and CPHF-GIAO approach for the NMR shielding constant computation using the Gaussian 03 program [29].

## 4.1. Syntheses

### 4.1.1. General procedure for the preparation of 3,3'-diindolylmethanes and 3,3'-diindolyl(aryl)methanes

Indole derivatives (5 mmol) were dissolved in water (25 ml) with an appropriate derivative of benzaldehyde (2.5 mmol) (for compounds of types **b** and **c**) or with formalin (0.20 g, 2.5 mmol) for compounds of type **a**. Next, 2 or 3 drops of concentrated H<sub>2</sub>SO<sub>4</sub> were added. The mixture was kept out of light and stirred at 85–100 °C for 2.5–5 h. The reaction was monitored by TLC. After reaching room temperature, the water phase was extracted three times with diethyl ether (10 ml) and the combined organic phases were dried with MgSO<sub>4</sub> anhydrous. The solvent was evaporated. The oily residue was recrystallized from benzene, hexane or alcohol. The

syntheses of 5,5'-diiodo-3,3'-diindolylmethane (**2a**) and 3,3'-diindolyl(4-methylphenyl)methane (**1b**) have been already described [16,18], but our procedure was more facile (it allowed us to avoid nitrogen and reduce the time of reaction). The structure of compound **2a** was additionally proved by X-ray diffraction measurement (melting points of **2a** in [16] and ours are very different). The synthesis of 4,4'-dimethoxy-3,3'-diindolylmethylum tetrafluoroborate was also given [30], but pure compound (**4a**) was not obtained until now.

**4.1.1.1. 5,5'-Diiodo-3,3'-diindolylmethane (2a) [16].** According to the general procedure pinkish solid was obtained. The compound was recrystallized from benzene to give 80% yield; mp = 148.5–148.8 °C. <sup>1</sup>H NMR (500 MHz, DMSO-*d*<sub>6</sub>),  $\delta$  in ppm: 4.08 (s, 2H, 10-H); 7.19 (s, 2H, 4-H, 4'-H); 7.21 (d, 2H, *J* = 8 Hz, 7-H, 7'-H); 7.29 (d, 2H, *J* = 8 Hz, 6-H, 6'-H); 7.85 (s, 2H, 2-H, 2'-H); 10.97 (s (broad), 2H, 2NH). <sup>13</sup>C NMR (125 MHz, DMSO-*d*<sub>6</sub>),  $\delta$  in ppm: 20.54 (C-10); 81.94 (C-5, C-5'); 113.39 (C-3, C-3'); 113.93 (C-7, C-7'); 124.07 (C-4, C-4'); 127.12 (C-2, C-2'); 128.71 (C-6, C-6'); 129.86 (C-8, C-8'); 135.45 (C-9, C-9'). Anal. Calcd for C<sub>17</sub>H<sub>12</sub>I<sub>2</sub>N<sub>2</sub> (498.10): C, 40.99%; H, 2.43%; I, 50.95%; N, 5.02%; found: C, 40.89%; H, 2.40%; N, 5.00%.

**4.1.1.2. 4,4'-Dimethoxy-3,3'-diindolylmethane (4a).** After general procedure and crystallization from benzene colourless solid of **4a** was obtained with 95% yield, mp = 161.3–162.5 °C. <sup>1</sup>H NMR (500 MHz, DMSO-*d*<sub>6</sub>),  $\delta$  in ppm: 3.82 (s, 6H, 2OCH<sub>3</sub>); 4.39 (s, 2H, 10-H); 6.42 (dd, 2H, *J*<sub>1</sub> = 1.5 Hz, *J*<sub>2</sub> = 7.0 Hz, 5-H, 5'-H); 6.75 (d, 2H, *J* = 2 Hz, 2-H, 2'-H); 6.90 (dd, 2H, *J*<sub>1</sub> = 1.5 Hz, *J*<sub>2</sub> = 7.0 Hz, 7-H, 7'-H); 6.92 (t, 2H, *J* = 7.0 Hz, 6-H, 6'-H); 10.63 (s (broad), 2H, 2NH); <sup>13</sup>C NMR (125 MHz, DMSO-*d*<sub>6</sub>),  $\delta$  in ppm: 22.22 (C-10); 54.55 (2OCH<sub>3</sub>); 98.29 (C-5, C-5'); 104.46 (C-7, C-7'); 115.61 (C-8, C-8'); 116.58 (C-3, C-3'); 121.05 (C-2, C-2'); 121.07 (C-6, C-6'); 137.46 (C-9, C-9'); 154.09 (C-4, C-4'). Anal. Calcd for C<sub>19</sub>H<sub>18</sub>N<sub>2</sub>O<sub>2</sub> (303.36): C, 74.49%; H, 5.92%; N, 9.14%; found: C, 74.29%; H, 5.91%; N, 8.99%.

**4.1.1.3. 3,3'-Diindolyl(4-methylphenyl)methane (1b) [18].** According to the general procedure colourless solid was obtained with 49% yield. Compound **1b** was recrystallized from benzene, mp = 87–87.3 °C. <sup>1</sup>H NMR (400 MHz, CDCl<sub>3</sub>),  $\delta$  in ppm: 2.35 (3H, 12''-H); 5.87 (s, 1H, 10-H); 6.63 (s, 2H, 2-H, 2'-H); 7.03 (t, 2H, 5-H, 5'-H, *J* = 8 Hz); 7.11 (d, 2H, *J* = 8 Hz, 13-H, 15-H); 7.19 (t, 2H, *J* = 8 Hz, 6-H, 6'-H); 7.25

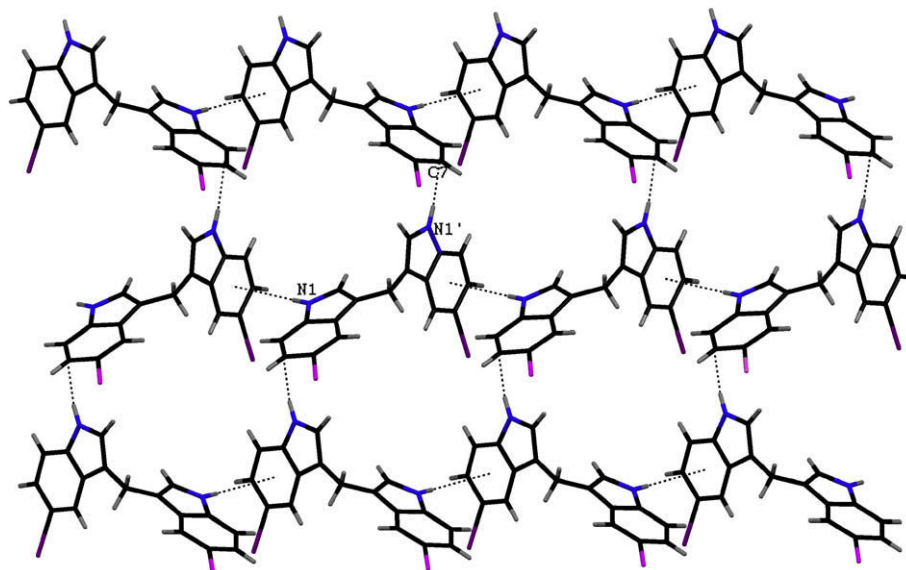


**Fig. 6.** The interconnections within a layer of **2a**.

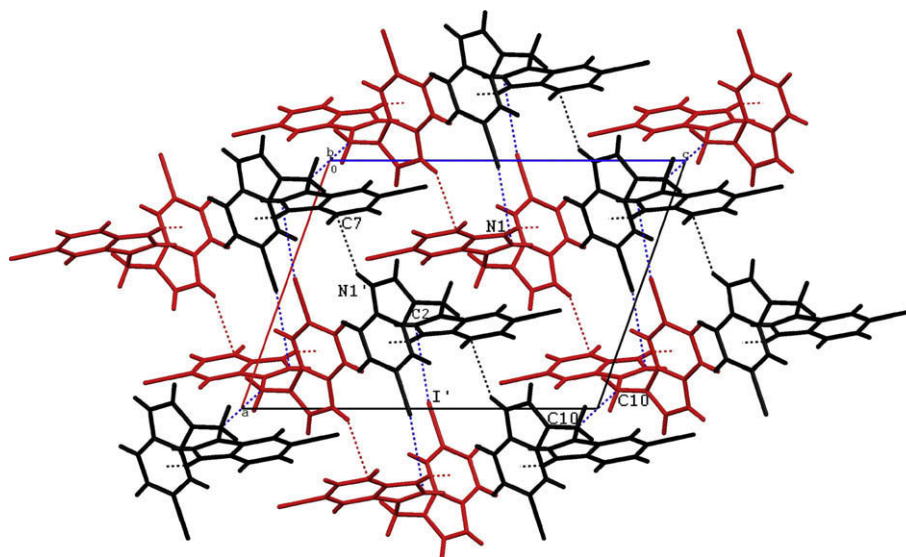


**Fig. 7.** Projection of the crystal structure of **2a** along the *b* axis with layers (black and red colours) and contacts (blue dashed lines) between them. (For interpretation of the references to colour in this figure legend, the reader is referred to the web version of the article.)

(m, 2H, 12-H, 16-H); 7.34 (d, 2H, 7-H, 7'-H,  $J = 8$  Hz); 7.42 (d, 2H, 4-H, 14-H,  $J = 8$  Hz); 7.80 (s (broad), 2H, 2NH);  $^{13}\text{C}$  NMR (100 MHz,  $\text{CDCl}_3$ ),  $\delta$  in ppm: 21.28 (C-12''); 39.95 (C-10), 111.20 (C-7, C-7'); 119.38 (C-5, C-5'); 120.07 (C-3, C-3'); 120.16 (C-4, C-4'); 122.06 (C-6, C-6'); 123.74 (C-2, C-2'); 127.29 (C-8, C-8'); 128.76 (C-12, C-16); 129.11 (C-13, C-15); 135.68 (C-14); 136.86 (C-9, C-9'); 141.18 (C-11).

#### 4.1.1.4. 5,5'-Diiodo-3,3'-diindolyl(4-methylphenyl)methane (**2b**).

According to the general procedure colourless solid of **2b** was obtained with 18% yield. Compound **2b** was recrystallized from benzene, mp = 224.7–225.0 °C.  $^1\text{H}$  NMR (400 MHz,  $\text{CDCl}_3$ ),  $\delta$  in ppm: 2.26 (s, 3H, 12''-H); 5.63 (s, 1H, 10-H); 6.52 (s, 2H, 2-H, 2'-H); 7.04 (m, 2H, 15-H, 13-H); 7.07 (d, 2H,  $J = 8$  Hz, 7-H, 7'-H); 7.34 (dd, 2H,  $J_1 = 8$  Hz,  $J_2 = 1.2$  Hz, 6-H, 6'-H); 7.61 (d, 2H,  $J_2 = 1.2$  Hz, 4-H, 4'-H); 7.87 (s (broad), 2H, 2NH).  $^{13}\text{C}$  NMR (100 MHz,  $\text{CDCl}_3$ ),  $\delta$  in ppm: 21.30 (C-12''); 39.56 (C-10); 83.14 (C-5, C-5'); 113.30 (C-7, C-7'); 119.24 (C-3, C-3'); 124.51 (C-2, C-2'); 128.55 (C-12, C-16); 128.75

(C-4, C-4'); 129.33 (C-13, C-15); 129.69 (C-8, C-8'); 130.62 (C-6, C-6'); 135.98 (C-9, C-9'); 136.15 (C-14); 140.24 (C-11). Anal. Calcd for  $\text{C}_{24}\text{H}_{18}\text{I}_2\text{N}_2$  (588.23): C, 49.01; H, 3.08; I, 143.15; N, 4.76; found: C, 48.96%; H, 3.11%; N, 4.75%.

#### 4.1.1.5. 5,5'-Dimethoxy-3,3'-diindolyl(4-methylphenyl)methane (**3b**).

After general procedure, colourless solid was recrystallized from methanol to give 60% yield of compound **3b**, mp = 215.4–215.7 °C.  $^1\text{H}$  NMR (400 MHz,  $\text{CDCl}_3$ ),  $\delta$  in ppm: 2.51 (s, 3H, 12''-CH<sub>3</sub>); 3.47 (s, 6H, 2OCH<sub>3</sub>); 5.67 (s, 1H, 10-H); 6.66 (dd, 2H,  $J_1 = 8$  Hz,  $J_2 = 1.2$  Hz, 6-H, 6'-H); 6.70 (d, 2H,  $J = 1.2$  Hz, 4-H, 4'-H); 6.78 (s, 2H, 2-H, 2'-H); 7.04 (m, 2H, 13-H, 15-H); 7.20 (m, 2H, 12-H, 16-H); 7.22 (d, 2H,  $J = 8$  Hz, 7-H, 7'-H); 10.60 (s, broad, 2H, 2NH).  $^{13}\text{C}$  NMR (100 MHz,  $\text{CDCl}_3$ ),  $\delta$  in ppm: 20.74 (C-11); 39.36 (C-10); 55.39 (2OCH<sub>3</sub>), 101.69 (C-4, C-4'); 110.62 (C-6, C-6'); 112.08 (C-7, C-7'); 118.00 (C-3, C-3'); 124.20 (C-2, C-2'); 127.15 (C-8, C-8'); 128.33 (C-12, C-16); 128.71 (C-13, C-15); 131.94 (C-9, C-9'); 134.70 (C-14); 142.08 (C-11); 152.76

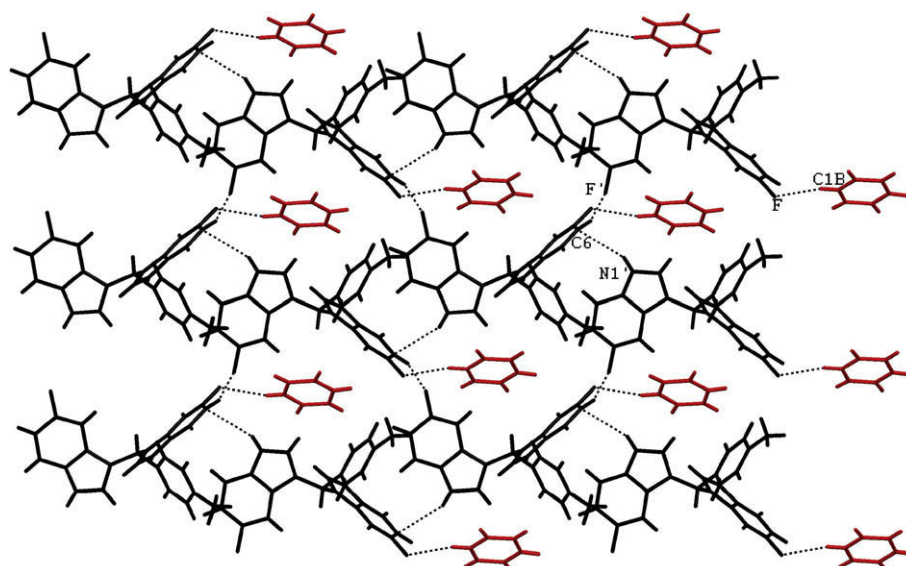


**Fig. 8.** The interconnections within the layer of **3b**.

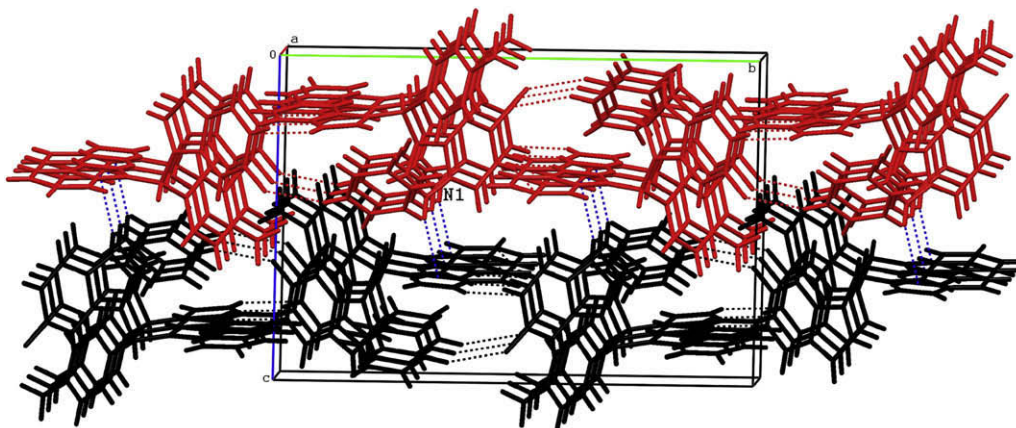


**Fig. 9.** Projection of the crystal structure of **8b** along the *a* axis with layers (black and red colours) and N1–H1... $\pi$  contacts (blue dashed lines) between them. (For interpretation of the references to colour in this figure legend, the reader is referred to the web version of the article.)

(C-5, C-5'). Anal. Calcd for  $C_{26}H_{24}N_2O_2$  (396.49): C, 78.76%; H, 6.10%; N, 7.07%; found: C, 78.37%; H, 6.06%; N, 7.00%.

**4.1.1.6. 5,5'-Dibromo-3,3'-diindolyl(4-methylphenyl)methane (7b).** After general procedure, colourless solid was recrystallized from benzene/hexane (1:2 v/v) to give 28% yield of compound **7b**, mp = 214.5–214.7 °C.  $^1H$  NMR (400 MHz,  $CDCl_3$ ),  $\delta$  in ppm: 2.20 (s, 3H, 12''-CH<sub>3</sub>); 5.56 (s, 1H, 10-H); 6.47 (s, 2H, 2-H, 2'-H); 6.95 (m, 2H, 13-H, 15-H); 7.03 (m, 2H, 12-H, 16-H); 7.05 (d, 2H,  $J = 8.5$  Hz, 7-H, 7'-H); 7.11 (dd, 2H,  $J_1 = 8.5$  Hz,  $J_2 = 1$  Hz, 6-H, 6'-H); 7.40 (s (broad), 2H, 4-H, 4'-H); 7.74 (s (broad), 2H, 2NH).  $^{13}C$  NMR (100 MHz,  $CDCl_3$ ),  $\delta$  in ppm: 21.27 (C-12''); 39.68 (C-10); 112.77 (C-7, C-7'); 112.85 (C-5, C-5'); 119.46 (C-3, C-3'); 122.50 (C-4, C-4'); 124.90 (C-2, C-2'); 125.13 (C-6, C-6'); 128.57 (C-12, C-16); 128.89 (C-8, C-8'); 129.34 (C-13, C-15); 135.54 (C-14); 136.16 (C-9, C-9'); 140.23 (C-11). Anal. Calcd for  $C_{24}H_{18}Br_2N_2 \cdot \frac{1}{2}C_6H_6$  (533.29): C, 60.81%; H, 3.97%; Br, 29.397%; N, 5.25%; found: C, 59.87%; H, 3.90%; N, 5.30%.

**4.1.1.7. 5,5'-Difluoro-3,3'-diindolyl(4-methylphenyl)methane (8b).** After general procedure, colourless solid was recrystallized from

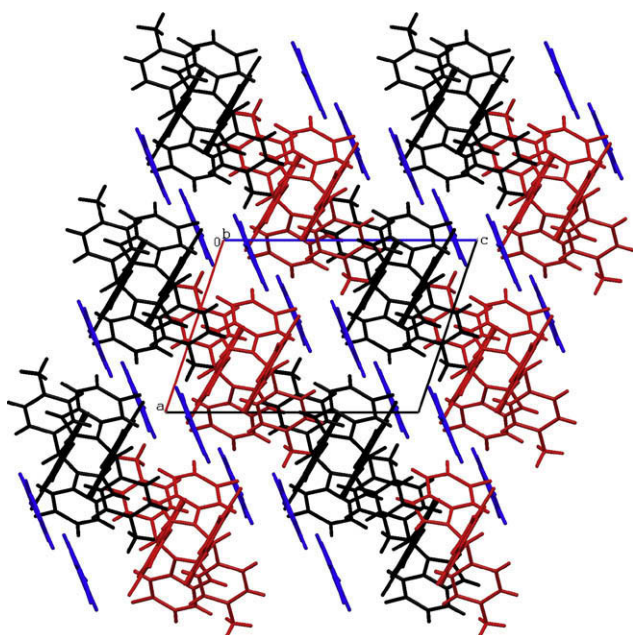


**Fig. 10.** The packing arrangement of **8b** along the *b* axis.

benzene to give 52% yield of compound **8b**, mp = 90.8–91.2 °C.  $^1H$  NMR (400 MHz,  $CDCl_3$ ),  $\delta$  in ppm: 2.30 (s, 3H, 12''-CH<sub>3</sub>); 5.65 (s, 1H, 10-H); 6.63 (d, 2H,  $J = 1$  Hz, 2-H, 2'-H); 6.87 (td, 2H,  $J_1 = 8.8$  Hz,  $J_2 = 2.0$  Hz, 6-H, 6'-H); 6.97 (dd, 2H,  $J_1 = 9.6$  Hz,  $J_2 = 2.0$  Hz, 4-H, 4'-H); 7.06 (m, 2H, 13-H, 15-H); 7.16 (m, 2H, 12-H, 16-H); 7.18 (d,  $J = 8.8$  Hz, 2H, 7-H, 7'-H); 7.76 (s (broad), 2H, 2NH).  $^{13}C$  NMR (100 MHz,  $CDCl_3$ ),  $\delta$  in ppm: 21.24 (C-12''); 40.00 (C-10); 104.96 (d,  $J_{C-F} = 23.3$  Hz, C-4, C-4'); 110.51 (d,  $J_{C-F} = 26.2$  Hz, C-6, C-6'); 111.50 (d,  $J_{C-F} = 6.8$  Hz, C-7, C-7'); 119.79 (d,  $J_{C-F} = 4.7$  Hz, C-3, C-3'); 125.38 (C-2, C-2'); 127.53 (d,  $J_{C-F} = 9.7$  Hz, C-8, C-8'); 128.62 (C-12, C-16); 129.28 (C-13, C-15); 133.36 (C-9, C-9'); 136.04 (C-14); 140.45 (C-11); 157.69 (d,  $J_{C-F} = 233$  Hz, C-5, C-5'). Anal. Calcd for  $C_{24}H_{18}F_2N_2 \cdot \frac{1}{2}C_6H_6$  (411.47) C, 78.81%; H, 5.14%; N, 6.781%; found: C, 78.42%; H, 5.27%; N, 6.49%.

**4.1.1.8. 3,3'-Diindolyl(3,5-difluorophenyl)methane (1c).** After general procedure, colourless solid was dissolved in ethanol and drops of water were slowly added at boiling point to give 54% yield of compound **1c**, mp = 159–160 °C.  $^1H$  NMR (400 MHz,  $CDCl_3$ ),  $\delta$  in ppm: 5.83 (s, 1H, 10-H); 6.59 (s, 2H, 2-H, 2'-H); 6.64 (tt, 1H,  $J_1 = 9$  Hz,  $J_2 = 2$  Hz, 14-H); 6.84 (m, 2H, 12-H, 16-H); 7.02 (t, 2H,  $J = 8$  Hz, H-5, H-5'); 7.18 (t, 2H,  $J = 8$  Hz, H-6, H-6'); 7.32 (d, 2H,  $J = 8$  Hz, H-7, H-7'); 7.36 (d, 2H,  $J = 8$  Hz, H-4, H-4'); 7.80 (s (broad), 2H, 2NH).  $^{13}C$  NMR (100 MHz,  $CDCl_3$ ),  $\delta$  in ppm: 40.23 (C-10), 101.97 (t, C-14,  $J_{C-F} = 25.4$  Hz); 111.45 (C-7, C-7'), 111.78 (tt, C-12, C-16,  $J_{C-F} = 24.6$  Hz), 118.56 (C-3, C-3'), 119.73 (C-5, C-5'), 119.86 (C-4, C-4'), 122.44 (C-6, C-6'), 123.81 (C-2, C-2'), 126.97 (C-8, C-8'), 136.88 (C-9, C-9'), 148.62 (t,  $J = 8.1$  Hz, C-11); 163.23 (dd, C-13, C-15,  $J_{C-F} = 246$  Hz,  $J_{C-F} = 12.7$  Hz). Anal. Calcd for  $C_{23}H_{16}F_2N_2$  (347.35) C, 77.08%; H, 4.50%; N, 7.82%; found: C, 77.07%; H, 4.45%; N, 7.88%.

**4.1.1.9. 5,5'-Diiodo-3,3'-diindolyl(3,5-difluorophenyl)methane (2c).** After general procedure, colourless solid was dissolved in benzene and drops of hexane were slowly added at boiling point to give 40% yield of compound **2c**, mp = 109.9–110.5 °C.  $^1H$  NMR (300 MHz,  $CDCl_3$ ),  $\delta$  in ppm: 5.70 (s, 10-H); 6.59 (d, 2H, 2-H, 2'-H,  $J = 1.5$  Hz); 6.69 (tt, 1H,  $J_1 = 9$  Hz,  $J_2 = 2$  Hz, 14-H); 6.79 (m, 2H, 12-H, 16-H); 7.14 (d, 2H,  $J = 9$  Hz, 7-H, 7'-H); 7.44 (dd, 2H,  $J_1 = 9$  Hz,  $J_2 = 1.5$  Hz, 6-H, 6'-H); 7.65 (d, 2H,  $J = 1.5$  Hz, 4-H, 4'-H); 7.97 (s (broad), 2NH).  $^{13}C$  NMR (75 MHz,  $CDCl_3$ ),  $\delta$  in ppm: 39.73 (C-10); 83.43 (C-5, C-5'); 102.42 (t,  $J_{C-F} = 25.2$  Hz, C-14); 111.64 (m, C-12, C-16); 113.50 (C-7', C-7'); 117.67 (C-3, C-3'); 124.57 (C-2, C-2'); 128.44 (C-4, C-4'); 129.34 (C-8, C-8'); 131.00 (C-6, C-6'); 135.97 (C-9, C-9'); 147.60 (t,  $J_{C-F} = 7.5$  Hz, C-11); 163.29 (dd,  $J_{C-F} = 246.9$  Hz,  $J_{C-F} = 12.6$  Hz, C-13, C-15). Anal. Calcd for  $C_{23}H_{14}F_2I_2N_2 \cdot C_6H_6$  (610.19) C, 50.61%; H, 2.93%; N, 4.07%; found: C, 50.81%; H, 2.99%; N, 4.09%.

**4.1.1.10. 5,5'-Dimethoxy-3,3'-diindolyl-(3,5-difluorophenyl)methane (3c).** After general procedure, colourless solid was recrystallized from methanol to give 60% yield of compound **3c**, mp = 195.4–196 °C. <sup>1</sup>H NMR (500 MHz, CDCl<sub>3</sub>), δ in ppm: 3.72 (s, 6H, 2OCH<sub>3</sub>); 5.74 (s, 1H, 10-H); 6.66 (tt (hidden), 1H, 14-H); 6.66 (d, 2H, J = 2 Hz, 2-H, 2'-H); 6.78 (d, 2H, J = 2.5 Hz, 4-H, 4'-H); 6.86 (dd, 2H, J<sub>1</sub> = 8.5 Hz, J<sub>2</sub> = 2.5 Hz, 6-H, 6'-H); 6.87 (dd, 2H, J<sub>1</sub> = 8.5 Hz, J<sub>2</sub> = 2.0 Hz, 12-H, 16-H); 7.25 (d, 2H, J = 8.5 Hz, 7-H, 7'-H); 7.86 (s (broad), 2H, 2NH). <sup>13</sup>C NMR (125 MHz, CDCl<sub>3</sub>), δ in ppm: 40.05 (C-10); 54.89 (2OCH<sub>3</sub>); 101.71 (t, J<sub>C-F</sub> = 20.7 Hz, C-14), 101.66 (C-4, C-4'); 111.53 (m, C-12, C-16); 111.86 (C-6, C-6'); 112.13 (C-7, C-7'); 117.92 (C-3, C-3'); 124.40 (C-2, C-2'); 127.17 (C-8, C-8'); 131.84 (C-9, C-9'); 148.34 (t, J<sub>C-F</sub> = 8.40 Hz, C-11); 153.89 (C-5, C-5'); 163.00 (dd, J<sub>C-F</sub> = 196.3 Hz, J<sub>C-F</sub> = 10.3 Hz, C-13, C-15). Anal. Calcd for C<sub>25</sub>H<sub>20</sub>F<sub>2</sub>N<sub>2</sub>O<sub>2</sub> (418.42): C, 71.76%; H, 4.82%; N, 6.69%; found: C, 71.69%; H, 4.88%; N, 6.70%.

**4.1.1.11. 5,5'-Dibromo-3,3'-diindolyl(3,5-difluorophenyl)methane (7c).** After general procedure, colourless solid was recrystallized from benzene/hexane (1:1, v/v) to give 19% yield of compound **7c**, mp = 118.7–119.3 °C. <sup>1</sup>H NMR (400 MHz, CDCl<sub>3</sub>), δ in ppm: 5.74 (s, 1H, H-10); 6.67 (d, 2H, J = 1.5 Hz, 2-H, 2'-H); 6.71 (tt, 1H, J<sub>1</sub> = 9.2 Hz, J<sub>2</sub> = 2 Hz, 14-H); 6.81 (m, 2H, 12-H, 16-H); 7.26 (d, 2H, J = 8.4 Hz, 7-H, 7'-H); 7.29 (dd, 2H, J<sub>1</sub> = 8.4 Hz, J<sub>2</sub> = 1.5 Hz, 6-H, 6'-H), 7.47 (d, 2H, J = 1.5 Hz, 4-H, 4'-H); 8.02 (s (broad), 2H, 2NH). <sup>13</sup>C NMR (100 MHz, CDCl<sub>3</sub>), δ in ppm: 39.78 (C-10); 102.35 (t, J = 25.2 Hz, C-14); 111.60 (m, C-12, C-16); 112.91 (C-7, C-7'); 113.12 (C-5, C-5'); 117.87 (C-3, C-3'); 122.14 (C-4, C-4'); 124.89 (C-2, C-2'); 125.47 (C-6, C-6'); 128.48 (C-8, C-8'); 135.47 (C-9, C-9'); 147.52 (t, J<sub>C-F</sub> = 8.40 Hz, C-11); 163.25 (dd, J<sub>C-F</sub> = 246.7 Hz, J<sub>C-F</sub> = 12.9 Hz, C-13, C-15). Anal. Calcd for C<sub>23</sub>H<sub>14</sub>Br<sub>2</sub>F<sub>2</sub>N<sub>2</sub>·C<sub>6</sub>H<sub>6</sub> (594.30): C, 58.61%; H, 3.39%; Br, 26.89%; F, 6.39%; N, 4.71%; found: C, 58.21%, H, 3.30%; N, 4.61%.

#### 4.2. X-ray diffraction measurements' details

Crystals of **2a** and **8b**, suitable for X-ray analysis, were grown by slow evaporation from benzene solution. All details of the measurements, crystal data and structure refinement are given in Table 4. The data were collected on an Oxford Diffraction KM4CCD diffractometer [31], using graphite-monochromated Mo K<sub>α</sub> radiation, at 293 K and 120 K for **2a** and **8b**, respectively. The unit cells parameters were determined by least-squares treatment of setting angles of highest-intensity reflections chosen from the whole experiments. Intensity data were corrected for the Lorentz and polarization effects [32]. The structures were solved by direct methods by use of the SHELXS97 program [33] and refined by the full-matrix least-squares method with the SHELXL97 program [34]. Three reflections for **2a** and two for **8b** were excluded from the reflection file due to their large ( $|F_o|^2 - |F_c|^2$ ) differences. The function  $\sum w(|F_o|^2 - |F_c|^2)^2$  was minimized with  $w^{-1} = [\sigma^2(F_o)^2 + (0.0388P)^2 + 1.0105P]$  for **2a** and  $w^{-1} = [\sigma^2(F_o)^2 + (0.1257P)^2 + 1.6736P]$  for **8b**, where  $P = (F_o^2 + 2F_c^2)/3$ . All non-hydrogen atoms were refined with anisotropic thermal parameters. The atoms of the benzene ring (of the solvent which is included in crystals of **8b**) appeared disordered, so restrains for the thermal parameters and the bond lengths for these atoms, according to SHELXL97, were applied. The coordinates of the hydrogen atoms were calculated in idealized positions and refined as a riding model with their thermal parameters calculated as 1.2 (1.5 for methyl group) times  $U_{eq}$  of the respective carrier carbon atom.

The deposition numbers CCDC 730183 for **2a** and 730184 for **8b** contain the supplementary crystallographic data for this paper. These data can be obtained free of charge via [www.ccdc.cam.ac.uk/data\\_request/cif](http://www.ccdc.cam.ac.uk/data_request/cif), or by emailing [data\\_request@ccdc.cam.ac.uk](mailto:data_request@ccdc.cam.ac.uk), or

**Table 4**  
Crystal data, data collection and structure refinement for compounds **2a** and **8b**.

Compound	<b>2a</b>	<b>8b</b>
Empirical formula	C <sub>17</sub> H <sub>12</sub> N <sub>2</sub> I <sub>2</sub>	C <sub>30</sub> H <sub>24</sub> N <sub>2</sub> F <sub>2</sub>
Formula weight	498.09	450.51
T (K)	293(2)	120(2)
Wavelength (Å)	0.71073	0.71073
Crystal system, space group	Monoclinic, P2 <sub>1</sub> /n	Monoclinic, P2 <sub>1</sub> /n
Unit cell dimensions		
a (Å)	11.6634(5)	9.8917(6)
b (Å)	9.0383(3)	19.4883(8)
c (Å)	15.7982(5)	13.7389(6)
β (°)	109.600(4)	108.628(6)
Volume (Å <sup>3</sup> )	1568.9(1)	2509.7(2)
Z, D <sub>x</sub> (Mg/m <sup>3</sup> )	4, 2.109	4, 1.192
μ (mm <sup>-1</sup> )	4.003	0.080
F(000)	936	944
θ range for data collection (°)	4.16–25.03	4.18–25.02
hkl range	–10 ≤ h ≤ 13 –10 ≤ k ≤ 10 –18 ≤ l ≤ 18	–11 ≤ h ≤ 11 –22 ≤ k ≤ 23 –16 ≤ l ≤ 16
Reflections		
Collected	9225	23 459
Unique (R <sub>int</sub> )	2754 (0.014)	4404(0.023)
Observed (I > 2σ(I))	2260	3253
Data/restraints/parameters	2754/0/190	4404/42/307
Absorption correction	Multi-scan	Multi-scan
Goodness-of-fit on F <sup>2</sup>	1.040	1.078
R(F) (I > 2σ(I))	0.0218	0.0676
wR(F <sup>2</sup> ) (all data)	0.0654	0.2208
Max/min. Δρ (e/Å <sup>3</sup> )	0.557/–0.719	0.849/–0.439

by contacting The Cambridge Crystallographic Data Centre, 12, Union Road, Cambridge CB2 1EZ, UK; fax: +44 1223 336033.

#### 4.3. Biological assays

##### 4.3.1. In vitro assays: chemicals, solutions and other materials

The cell culture flasks and the 96-well microplates were provided by Nunc. MTT: 3-(4,5-dimethylthiazol-2-yl)-2,5-diphenyltetrazolium bromide, DMSO (dimethyl sulfoxide) and antimycotic antibiotics (penicillin and streptomycin) were obtained from Sigma Co. MEM (Minimum Essential Medium) was purchased from Gibco Co. PBS (phosphate–Ca<sup>2+</sup> and Mg<sup>2+</sup>-free buffered saline) was obtained from IITD, Poland. Fetal bovine serum was bought from Bioproduct, Hungary. The stock solutions of tested compounds were freshly prepared in DMSO and diluted in medium just before use. In the final dilutions obtained the concentrations of DMSO never exceeded 0.4%.

**Table 5**  
The IC<sub>50</sub> values of the tested compounds (in μmol/ml, x ± SEM).

Compound	WS1-human embryonic skin fibroblasts	ME18-human melanoma	ME18/R-human melanoma/resistant to doxorubicin
<b>1a</b>	36.6 ± 6.5	37.0 ± 0.4	40.7 ± 2.0
<b>2a</b>	13.0 ± 1.0	9.7 ± 2.7	17.3 ± 4.0
<b>3a</b>	22.8 ± 4.9	21.2 ± 6.5	30.7 ± 7.8
<b>4a</b>	31.0 ± 3.3	21.2 ± 7.8	22.5 ± 4.2
<b>5a</b>	32.7 ± 4.3	23.6 ± 4.8	19.7 ± 4.6
<b>6a</b>	33.3 ± 3.6	16.9 ± 5.8	14.3 ± 4.0
<b>1b</b>	58.4 ± 4.0	46.7 ± 1.9	35.9 ± 4.9
<b>2b</b>	16.2 ± 3.6	22.6 ± 3.1	21.1 ± 6.8
<b>3b</b>	38.6 ± 6.3	32.9 ± 6.6	33.0 ± 1.5
<b>7b</b>	26.3 ± 2.8	18.0 ± 1.9	17.4 ± 5.7
<b>8b</b>	45.9 ± 9.9	43.0 ± 1.2	32.5 ± 10.5
<b>1c</b>	36.0 ± 2.0	31.1 ± 4.6	17.0 ± 5.2
<b>2c</b>	28.5 ± 1.7	21.3 ± 1.1	23.8 ± 2.1
<b>3c</b>	26.5 ± 7.9	28.4 ± 0.9	28.2 ± 5.0
<b>7c</b>	24.2 ± 2.9	23.4 ± 2.9	22.7 ± 5.4

#### 4.3.2. Cell lines and culture conditions

The cell lines WS1 (human embryonic skin fibroblasts) were supplied by ATCC, ME18 (human melanoma cells) was a gift from M. Skłodowska-Curie Memorial Cancer Center and Institute of Oncology, Warsaw, Poland, ME18/R (the subline resistant to doxorubicin) was obtained experimentally in National Medicines Institute [35]. Cells are also resistant to vinblastine and methotrexate, which indicates that they have acquired pattern of pleiotropic multidrug resistance [36]. Cells were cultured as monolayers in MEM medium supplemented with 10% fetal bovine serum and antibiotics in humidified atmosphere at 37 °C and 5% CO<sub>2</sub>. The cell line ME18/R was maintained in MEM with doxorubicin, 0.04 μM. All cell cultures were mycoplasma-free.

#### 4.3.3. MTT assay

Cell survival was evaluated by using the MTT-dye reduction assay, which is based on the ability of viable cells to metabolize a yellow tetrazolium salt to violet formazan product that can be detected spectrophotometrically. The assay was carried out by the method previously described [37] with minor modifications [38].

The suspension of cells was diluted in MEM to concentration of 10<sup>5</sup> cells/ml and 0.05 ml of suspension was placed into individual well on 96-well multiplate. Then, 0.05 ml of the tested compounds solved in DMSO and diluted in MEM were added at double strength dilution. After a 48 h continuous exposure the medium was removed and 50 μl of MTT solution in PBS (5 mg/ml) was added. The plates were incubated for 4 h at 37 °C in a humidified 5% CO<sub>2</sub> atmosphere. The formazan crystals yielded were dissolved in DMSO and the absorbance was measured at 500 nm. The final concentration of *bis*-indole derivatives ranged from 1.25 to 30 μg/ml. The cells treated as control were kept in *bis*-indole-free medium or in medium with DMSO. In all experiments, three replicate wells were used at each point. IC<sub>50</sub> values were determined graphically and analyzed statistically by the ANOVA test.

#### Acknowledgments

The authors thank Interdisciplinary Center for Mathematical and Computational Modeling (ICM) of Warsaw University for the computational grant.

#### References

- [1] R.H. Dashwood, A.T. Fong, D.E. Williams, J.D. Hendricks, G.S. Bailey, *Cancer Res.* 51 (1991) 2362–2365.
- [2] D.J. Kim, B.S. Han, B. Ahn, R. Hasegawa, T. Shirai, N. Ito, H. Tsuda, *Carcinogenesis* 18 (1997) 377–381.
- [3] C.A. De Kruif, J.W. Marsman, J.C. Venekamp, et al., *Chem. Biol. Interact.* 80 (1991) 305–315.
- [4] I. Chen, A. McDougal, F. Wang, S. Safe, *Carcinogenesis* 19 (1998) 1631–1639.
- [5] X. Chang, J.C. Tou, C. Hong, et al., *Carcinogenesis* 26 (2005) 771–778.
- [6] M. Nachshon-Kedmi, F.A. Fares, S. Yannai, *Prostate* 61 (2004) 153–160.
- [7] C. Hong, H.A. Kim, G.L. Firestone, et al., *Carcinogenesis* 23 (2002) 1297–1305.
- [8] C. Hong, G.L. Firestone, L.F. Bjeldanes, *Biochem. Pharmacol.* 63 (2002) 1085–1097.
- [9] L. Xue, G.L. Firestone, L.F. Bjeldanes, *Oncogene* 24 (2005) 2343–2353.
- [10] Y. Gong, H. Sohn, L. Xue, G.L. Firestone, L.F. Bjeldanes, *Cancer Res.* 66 (2006) 4880–4887.
- [11] M.A. Zelig, C. Jacobs, *Formulation and Use of Controlled Release Indole Alkaloids*, US Patent 6,416,793; 9.07.2002.
- [12] H. Shirani, B. Stensland, J. Bergman, T. Janosik, *Synlett* 15 (2006) 2459.
- [13] H. Shirani, T. Janosik, *Synthesis* 17 (2007) 2690.
- [14] A. McDougal, M.S. Gupta, K. Ramamoorthy, G. Sun, S.H. Safe, *Cancer Lett.* 151 (2000) 169.
- [15] P.K. Pradhan, S. Dey, V.S. Giri, P. Jaisankar, *Synthesis* (2005) 1779–1782.
- [16] S. Fóldeak, J. Czombos, B. Matkowsics, *Acta Univ. Sjedged. Acta Phys. Chem.* 11 (1965) 115–125.
- [17] C. Pal, S. Dey, S.K. Mahato, J. Vinayagam, P.K. Pradhan, V.S. Giri, P. Jaisankar, T. Hossain, S. Baruri, D. Ray, S.M. Biswas, *Bioorg. Med. Chem. Lett.* 17 (2007) 4924–4928.
- [18] S.J. Ji, S.Y. Wang, Y. Zhang, T.P. Loh, *Tetrahedron* 60 (2004) 2051–2055.
- [19] R. Nagarajan, P.T. Perumal, *Chem. Lett.* 33 (2004) 288–289.
- [20] J. Haleblan, W. McCrane, *J. Pharm. Sci.* 58 (1969) 911–929.
- [21] D.C. Apperley, R.A. Fletton, R.K. Harris, R.W. Lancaster, S. Tavener, T.L. Threlfall, *J. Pharm. Sci.* 88 (1999) 1275.
- [22] A. Bauer-Brandl, *Int. J. Pharm.* 140 (1996) 195.
- [23] R.H. Harris, *J. Pharm. Pharmacol.* 59 (2007) 225–239.
- [24] D. Maciejewska, M. Niemyjska, I. Wolska, M. Włostowski, M. Rasztawicka, *Z. Naturforsch.* 59b (2004) 1137–1142.
- [25] M. Rasztawicka, I. Wolska, D. Maciejewska, *J. Mol. Struct.* 831 (2007) 174–179.
- [26] C.F. Macrae, P.R. Edgington, P. McCabe, E. Pidcock, G.P. Shields, R. Taylor, M. Towler, J. van de Streek, *Mercury: visualization and analysis of crystal structures*, *J. Appl. Crystallogr.* 39 (2006) 453.
- [27] D. Maciejewska, I. Wolska, M. Niemyjska, P. Żero, *J. Mol. Struct.* 753 (2005) 53–60.
- [28] HyperChem 7.01, Hypercube Inc., Canada, 2002.
- [29] M.J. Frisch, G.W. Trucks, H.B. Schlegel, G.E. Scuseria, M.A. Robb, J.R. Cheeseman, J.A. Montgomery Jr., T. Vreven, K.N. Kudin, J.C. Burant, J.M. Millam, S.S. Iyengar, J. Tomasi, V. Barone, B. Mennucci, M. Cossi, G. Scalmani, N. Rega, G.A. Petersson, H. Nakatsuji, M. Hada, M. Ehara, K. Toyota, R. Fukuda, J. Hasegawa, M. Ishida, T. Nakajima, Y. Honda, O. Kitao, H. Nakai, M. Klene, X. Li, J.E. Knox, H.P. Hratchian, J.B. Cross, C. Adamo, J. Jaramillo, R. Gomperts, R.E. Stratmann, O. Yazyev, A.J. Austin, R. Cammi, C. Pomelli, J.W. Ochterski, P.Y. Ayala, K. Morokuma, G.A. Voth, P. Salvador, J.J. Dannenberg, V.G. Zakrzewski, S. Dapprich, A.D. Daniels, M.C. Strain, O. Farkas, D.K. Malick, A.D. Rabuck, K. Raghavachari, J.B. Foresman, J.V. Ortiz, Q. Cui, A.G. Baboul, S. Clifford, J. Cioslowski, B.B. Stefanov, G. Liu, A. Liashenko, P. Piskorz, I. Komaromi, R.L. Martin, D.J. Fox, T. Keith, M.A. Al-Laham, C.Y. Peng, A. Nanayakkara, M. Challacombe, P.M.W. Gill, B. Johnson, W. Chen, M.W. Wong, C. Gonzalez, J.A. Pople, *Gaussian 03, Revision B.02*, Gaussian, Inc., Pittsburgh, PA, 2003.
- [30] U. Pindur, H. Witzel, *Monatsh. Chem.* 121 (1990) 77–80.
- [31] Oxford Diffraction Poland, CrysAlisCCD, CCD Data Collection GUI, Version 1.171.31.8 (2007) and 1.171.32.5 (2007).
- [32] Oxford Diffraction Poland, CrysAlisRED, CCD Data Reduction GUI, Version 1.171.31.5 (2006) and 1.171.32.5 (2007).
- [33] G.M. Sheldrick, *Acta Crystallogr.* A46 (1990) 467–473.
- [34] G.M. Sheldrick, *SHELXL97, Program for the Refinement of Crystal Structures*, University of Göttingen, Germany, 1997.
- [35] E.L. Anuszevska, B.M. Gruber, J.H. Kozirowska, *Biochem. Pharmacol.* 54 (1997) 597–603.
- [36] E.L. Anuszevska, J.H. Kozirowska, *Mutat. Res.* 431 (1999) 25–30.
- [37] T. Mosmann, *J. Immunol. Methods* 65 (1983) 55–60.
- [38] B.M. Gruber, E.L. Anuszevska, *Toxicol. In Vitro* 16 (2002) 663–667.